# NJC

Accepted Manuscript


This is an *Accepted Manuscript*, which has been through the Royal Society of Chemistry peer review process and has been accepted for publication.

*Accepted Manuscripts* are published online shortly after acceptance, before technical editing, formatting and proof reading. Using this free service, authors can make their results available to the community, in citable form, before we publish the edited article. We will replace this *Accepted Manuscript* with the edited and formatted *Advance Article* as soon as it is available.

You can find more information about *Accepted Manuscripts* in the Information for Authors.

Please note that technical editing may introduce minor changes to the text and/or graphics, which may alter content. The journal's standard Terms & Conditions and the Ethical guidelines still apply. In no event shall the Royal Society of Chemistry be held responsible for any errors or omissions in this *Accepted Manuscript* or any consequences arising from the use of any information it contains.

ROYAL SOCIETY OF CHEMISTRY

www.rsc.org/njc

# Rapid early formation and crystal refinement of chemical conversion hopeite coatings induced by substrate sandblasting

**Xian Zhang[a,b], Gui-yong Xiao[a,b], Xing-chuan Zhao [a,b], Kun He [a,b], Wen-hua Xu [a,b], Yu-peng Lu[a,b*]**

[a] Key Laboratory for Liquid-Solid Structural Evolution and Processing of Materials, Ministry of Education, Shandong University, Jinan, 250061, China;

[b] School of Materials Science and Engineering, Shandong University, Jinan, 250061, China.

[*]Corresponding author: Tel: 86-0531-88395966; Fax: 86-0531-88395966.

E-mail address: biosdu@sdu.edu.cn (Y. P. Lu)

## Abstract

Hopeite coating has attracted more attention recently, because of its corrosion resistance and functional properties. In this research, the influence of sandblasting on microstructure, phase and electrochemical behavior of the hopeite coatings are discussed. It is shown that both coatings formed on sandblasted (SB) and non-sandblasted (NSB) substrates are composed of hopeite and minor phosphophyllite. Sandblasting treatment significantly decreases crystal size and increases coating mass within a PCC period of 30 min. The electrochemical analysis reveals that sandblasting treatment of substrate can significantly improve the corrosion resistance of the samples in 0.9 wt. % sodium chloride solution. Adhesive test indicated that the PCC coating was strongly attached on the substrate.

**Keywords**：Stainless steel; Sandblasting; Hopeite; Chemical conversion; Corrosion resistance;

## 1. Introduction

Biomedical metals such as titanium (Ti), Ti alloys, stainless steels (SS) and Co-Cr alloys have been widely used in clinic, which can provided many solutions to the problems in the dental and orthopedic wound [1-3]. Although they are known to be corrosion resistance and thus biocompatible, they undergo corrosion in the aggressive body fluid [1]. For example, pitting corrosion, crevice corrosion, galvanic corrosion and fretting corrosion may occur on SS in simulated and actual physiological liquids [3, 4]. It might be predicted that the undesirable ions release into the peri-prosthetic environment is the potential result.

Biocompatibility and long-term effectiveness of implants depend to a great extent on their corrosion. Various surface modification technologies have been developed to achieve satisfactory surface performances of implant. According to the formation mechanism of the modified layer, they are roughly classified into mechanical, chemical, and physical methods, such as sandblasting [5], electrodepositing [6], and ion implantation [7], respectively. And many of them have been clinically used. However, many limitations still exist on the utilization of the reported surface modification methods, such as interfacial separation, torsion of the substrate, spallation and cracking of compound layer and so on [1]. Typically, the use of hydroxyapatite (HA) coating on implants is not out of question, especially in terms of long-term effectiveness [8, 9]. As a result, new surface modification methods should be introduced to improve the surface properties of biomedical alloys, perhaps with adopt of novel methods or transfer of engineering approaches.

Phosphate chemical conversion (PCC) is known as a metal pretreatment process to facilitate further coating or painting, and improve corrosion and/or wear resistance of the treated products, and it has advantages such as low-cost, rapid coating formation, easy operation, and suitability for coating on irregular surfaces. Besides, the formed PCC coating is continuous and highly adherent to the substrate [10]. In particular, hopeite ($Zn_3(PO_4)_2$ $4H_2O$), a main phase of zinc PCC coating, has recently been considered to be biocompatible and osteogenic as well as considered as a potential versatile biomedical material [11, 12]. It is of special significance that the PCC coating can be porous or dense with various crystal shapes and microstructure, showing promising application to establish cell or tissue responsive surface with micro- and nano-scale topography [13-15]. So, how to regulate phase composition, crystal size and shape of coating is of great importance.

Both Ti and SS are difficult to get a phosphate coating by the PCC method, due to the presence of a passive oxide layer on their surfaces. For this, a hydrothermal treatment at 250 ℃ for 6-8 h has been adopted to fabricate PCC coatings on Ti [16, 17]. Several methods such as substrate nitriding, electrochemical phosphating and hydrothermal treatment were adopted to fabricate PCC coatings on SS [18-20]. In previous work [21-24], we developed facile methods to fabricate PCC hopeite coating on Ti and SS with ultrasonic assistance or Fe curing as well as the influence of process parameters were studied. It is suggested that the metal or alloys with inert surface could be successfully chemical conversed when the surface are activated by chemical, plasma or mechanical effects [18].

Sandblasting is a commonly used method of mechanical cleaning. At the same time, sandblasting leads to increase of surface roughness, as well as the changes of surface energy, surface stress and surface charge, et al [5, 25, 26]. This may influence formation of

PCC coating and its microstructure as well as properties. In this paper, we report the fabrication of hopeite coating on SS substrate by the PCC method. The effect of substrate sandblasting on phase and microstructure of the coatings are investigated. The polarization curves of the samples are also examined.

## 2. Materials and method

### 2.1 Substrate and pretreatment

Commercially obtained 304 SS samples with the size of 10 × 10 × 1 $mm^3$, having the composition (wt. %) Cr: 18.43, Ni: 8.12, Mn: 1.52, Si: 0.42, P: 0.023, C: 0.059, S: 0.021 and Fe: balance, were used as substrates. Sandblasted (SB) samples were prepared by an air blast machine using $Al_2O_3$ particles for 10 s, while non-sandblasted (NSB) samples were also studied as the control group. The samples were degreased in an 80 g/L NaOH solution at 60 ℃ for 15 min, followed by pickling in a 30%V/V of HCl at room temperature for 1 min. Afterwards, activation was performed in a solution of 3 g/L Ti colloids ($Na_4TiO(PO_4)_2$, commercially obtained) at room temperature for 30 s.

### 2.2 Chemical conversion

Both the substrates were immersed in a bath with the composition of ZnO: 25 g/L, $H_3PO_4$ (85%): 8 ml/L, $HNO_3$: 30 ml/L, Ni $(NO_3)_2$: 0.2 g/L, Ca $(NO_3)_2$: 5 g/L and $C_6H_8O_7$: 5 g/L at 75 ℃ for 1.5 min, 3 min and 30 min, respectively. Before the immersion process, the bath solution, with the pH value of 2.0, was cured with a 5 g/L pure iron powder (AR, 98%) at room temperature for 24 h. The coated samples were dried in air for 24 h and kept in a desiccator for further characterization.

### 2.3 Characterization

A digital scale with an accuracy of ± 0.1 mg was used for the determination of the mass of samples.

The coating mass ($M$, g/m$^2$) was calculated according to Equation (1):

$$M = (m_1 - m_2)/A \quad (1)$$

where $m_1$ and $m_2$ are the weights (g) of the samples before and after the coatings were stripped, respectively, and $A$ is the area of the substrates (m$^2$). The stripping medium contained 50 g/L of chromium trioxide and the process was performed at 70 ℃ for 10 min. An eddy current thickness gauge was used to determine the thickness of the coating. The results of coating mass and thickness were both the respective average values of four different measurements.

The microstructures of the coatings were observed using a SU-70 field emission SEM (FE-SEM) equipped with an energy dispersive spectrometer (EDS). Atomic force microscope (AFM) analysis was performed using Dimension Icon scanning probe microscope (SPM). The phase analysis of the coatings was examined by a Rigaku D/max-γB X-ray diffractometer (XRD), with a CuKα radiation.

### 2.4 Electrochemical measurements

The corrosion behavior of the SB and NSB samples were evaluated by the electrochemical potentiodynamic polarization in a 0.9 wt. % sodium chloride solution which were carried out using a classical three electrodes the uncoated and coated samples with an exposed area of 1 cm$^2$ as working electrode. The potentiodynamic

curves were obtained using a Parstat potentiostat model 2273 at constant voltage scan rate of 1 mV/s.

### 2.5 Adhesion test

The tensile strength tests were carried out to obtain the adhesive bond strength of the PCC coating to the substrates, according to the modified ASTM C633-01 method [23]. Both sides of the coated samples were adhered by modified acrylic adhesive to stainless steel cylinders with 10 mm diameter. The tensile strength tests were carried out at a loading speed of 0.5 mm/min on a RGD-5 electric tension machine at room temperature. The adhesive bond strength was determined from the maximum load recorded. At least ten parallel samples were used and the adhesive strength was the average of five steady results among the ten samples. The standard deviation was also quoted.

## 3. Results and discussion

### 3.1 Phase analysis

Fig. 1 shows the XRD patterns of PCC coatings on 304 SS substrates, obtained at 75 ℃ for 3 and 30 min, respectively. It can be seen that the coatings are mainly composed of hopeite (JCPDS # 33-1474) with minor phosphophyllite (JCPDS # 29-1427). All of the coatings have similar phase spectra, although with various relative peak intensities. The relative intensities of phase peaks increased with duration time and those of substrates decrease, indicating the continuous formation of coatings. Meanwhile, the narrow and intense peaks of the coatings indicate a high crystallinity.

Amorphous hump is found at 2θ of 15-25° in inserted XRD pattern of the coating

treated for 3 min on NSB substrate (Fig. 1b, the inserted image), and it disappears with the increase of duration time (Fig. 1d), which suggests the existence of amorphous phase during the coating formation and its crystallization with the increase of processing time. The amorphous precipitation is one of the stages among the formation of PCC coating, followed by crystallization and growth of the crystals [27]. The amorphous hump in the coating formed after 3 min treatment on NSB substrate may come from incomplete crystallization of the amorphous precipitate formed at the earlier stage of coating formation. At the next stage, crystallization and growth of the coating will be involved from the amorphous phase [28]. In addition, there is no amorphous hump found from XRD patterns of coatings on SB substrates for all duration times (Fig. 1 a, c). It is clear that sandblasting treatment of substrates enhanced earlier crystallization through comparison of XRD patterns of the coatings formed on SB and NSB substrates at the same duration time of 3 min (Fig. 1 a, b, the inserted image). This might also be related to sandblasting treatment induced rapidly coating formation.

Compared with the XRD patterns of coatings on SB substrates, the diffraction intensities of the peak of coatings on NSB substrates along the (020) and (040) planes (Fig. 1b, d) are obviously high, which implies the preferred epitaxial growth of hopeite along the planes. The XRD patterns of the coatings formed on SB substrates show obviously lower peak intensities, which might be attributed to the increase of crystal nucleation rate and crystal refinement induced by sandblasting treatment of substrates. On the other hand, the lower peak intensities of the SB samples show the coating with

finer crystals.

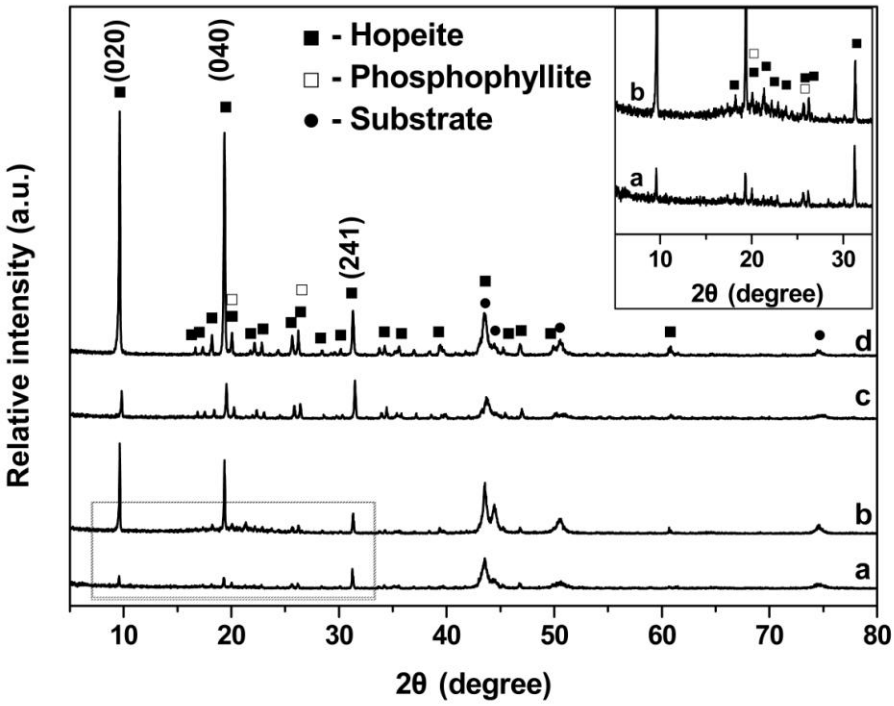


Fig. 1 XRD patterns of 304 SS samples PCC treated at 75 ℃ for 3 and 30 min. (a) 3 min, SB substrate, (b) 3 min, NSB substrate, (c) 30 min, SB substrate, (d) 30 min, NSB substrate. The inserted image shows local high magnification.

Hopeite is regarded as a potential versatile biomedical material due to high osteogenic property and good biocompatible [12, 21, 29]. It is reported that *in vitro* cell study shows that the osteogenic cells proliferation results for Ti-Zn-$PO_4$ coating are better than those for Ti bare substrate [17]. Moreover, based on previous work, human fibroblast cells attach and spread well on the surface of PCC coatings on Ti substrate [22]. The cell culture studies indicated the hopeite coatings have excellent biocompatibility and bioactivity. Hopeite is also widely used as anticorrosive pigments in industry.

Phosphophyllite possesses more chemical stability than hopeite in sodium chloride solution or other aqueous media, which is beneficial for the corrosion resistance of the coating [10, 30].

### 3.2 Microstructure

FE-SEM micrographs of the SB and NSB substrates are presented in Fig. 2. SB treatment leads to coarser texture on the substrate surface compared to grinding treatment using a 240-grit emery paper. On the NSB substrate, grooves that have arisen from the grinding process can be visualized (Fig. 2 a). The surface of SB substrate is covered with irregular scratches that it is very coarse and scraggy. After sandblasting treatment, the physical and chemical properties of the substrate surface, such as the surface energy, surface stress and surface charge, will be changed [5, 25, 26].

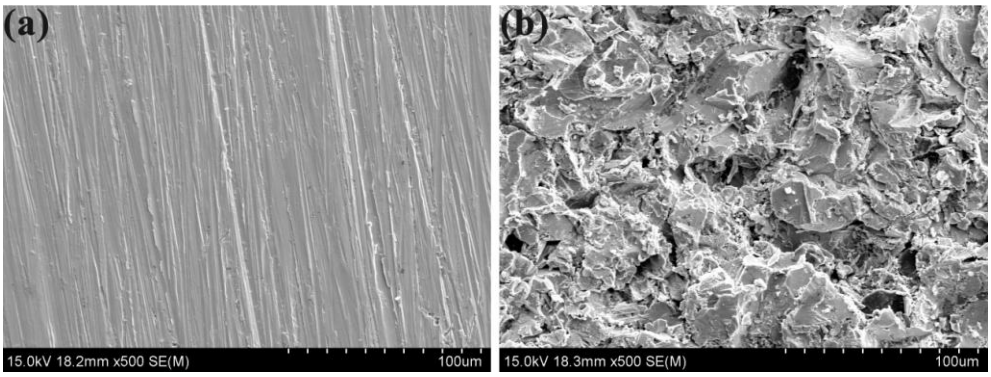


Fig. 2 FE-SEM images of 304 SS substrates after grinding treatment (a) and after sandblasting treatment (b).

FE-SEM micrographs of PCC coatings on SB and NSB substrates treated at 75 ℃ for 1.5 min, 3 min and 30 min are presented in Fig. 3. Figure 4 shows the local high magnification in Fig. 3a and b. It is obvious that the coatings exhibit fine structure with

plate-like (Fig. 3a-d) and vermiform (Fig. 3f) crystals with different dimension sizes. A continuous coating fully covered the whole SB substrates after 1.5 min treatment, whereas the NSB substrate is fully covered just after 30 min of PCC process treatment (Fig. 3 and 4). From Fig. 3b, d and f, it can also be clearly seen that the coatings formed on SB substrates have a crystal size of about 5-10 μm, which is obviously much smaller than that in the coatings formed on NSB substrates, with a crystal size of about 10-30 μm. Within conversion time of 1.5-3 min, plenty of crystallites are formed and fully covered SB substrate (Fig. 3a-d, Fig. 4), indicating that sandblasting treatment can enhance the nucleation of crystals.

After 30 min treatment, the NSB substrate surface is completely covered. At the same time, the crystals configuration of coating changes from plate-like (Fig. 3a, c) to net-like (Fig. 3e), while that on SB substrates changes from plate-like (Fig. 3b, d) to vermiform (Fig. 3f). Fig. 5 shows the EDS spectra of coatings PCC treated for 30 min on NSB (Fig. 5a) and SB substrates (Fig. 5b), indicating that O, Fe, Zn and P are the dominant elements on the surface of coatings. The result is in good agreement with the results of XRD (Fig. 1). And there is no element from substrate, suggesting that the thicknesses of coatings are thick enough.

The coating mass ($14.73 \pm 0.76$ g/m$^2$) and thickness ($10.13 \pm 0.81$ μm) of coatings on SB substrates are higher than those of NSB specimens, being $11.45 \pm 0.75$ g/m$^2$ and $8.76 \pm 0.54$ μm, indicating rapid formation of hopeite coating was induced by substrate sandblasting.

It is known that sandblasting leads to increase of the surface roughness (Fig. 2b) and surface energy, which can produce a great number of active centers and result in a high rate of nucleation [10, 25, 27]. Moreover, the SB surface could generate a negative electric charge by triboelectric effect [5], which can accelerate the diffusion of $Fe^{2+}$ and $Zn^{2+}$ from solution to the substrate/solution interface and enhance the formation of crystals [10]. After sandblasted treatment, the substrate of strong activity makes the precipitation of crystals [27]. In addition for crystal refinement, the increased nucleation rate will increase the coating formation rate and improve the coating uniformity (Fig. 3 b, d and f). Therefore, coating mass and thickness of coatings on SB substrates are higher. During the crystalline reorganization stage, which is the last stage of PCC treatment, the dissolution and reorganization of crystals are very rapid [27]. And the crystal configurations on SB and NSB substrates become net-like (Fig. 3 e) and vermiform (Fig. 3 f), respectively.

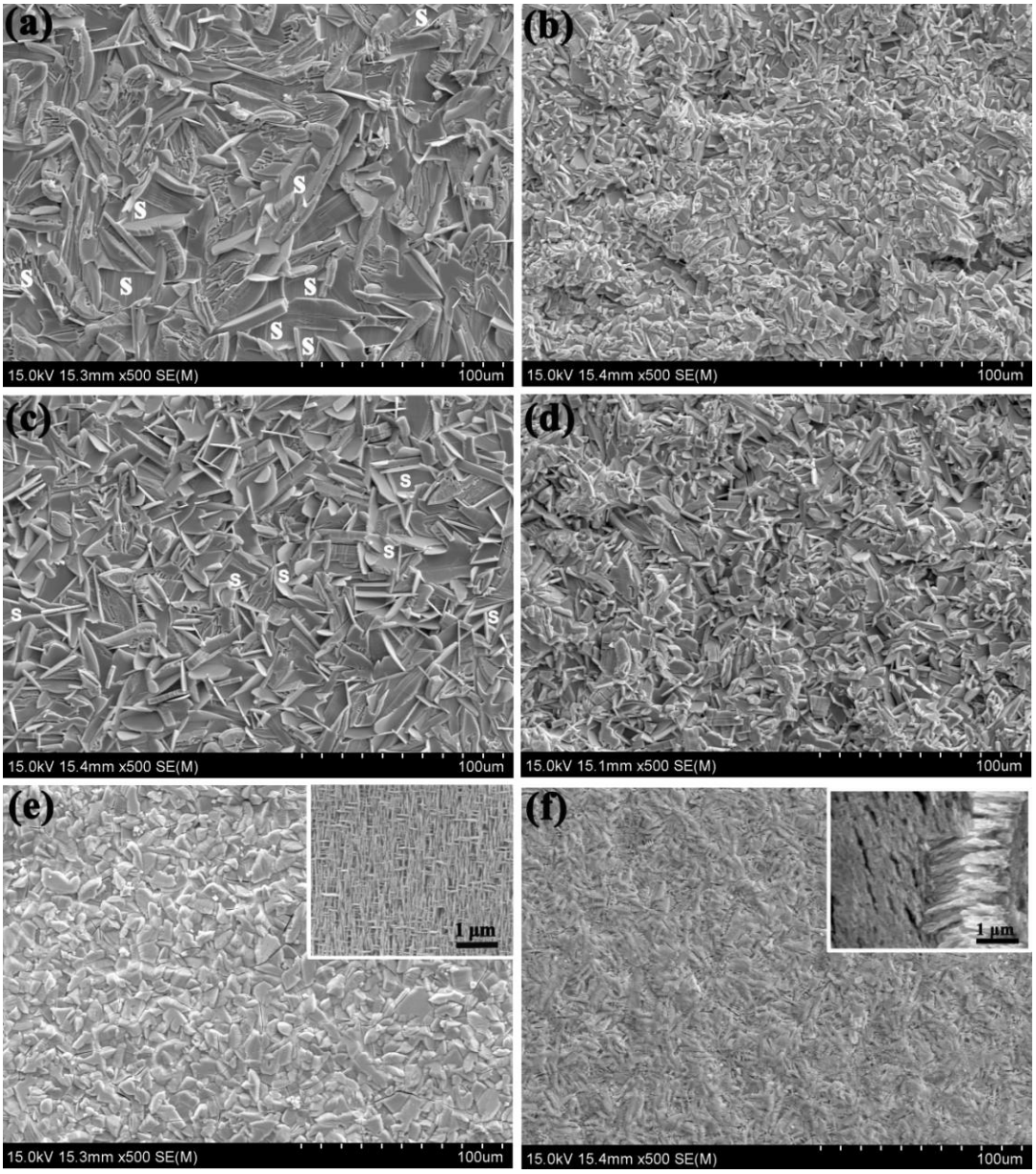


Fig. 3 FE-SEM images of 304 SS samples PCC treated at 75 ℃ for different times SB and NSB substrates. (a) 1.5 min, NSB substrate, (b) 1.5 min, SB substrate, (c) 3 min, NSB substrate, (d) 3 min, SB substrate, (e) 30 min, NSB substrate, (f) 30 min, SB substrate. (S: Substrate). The inserted images show the typical fine structure of the crystal surfaces.

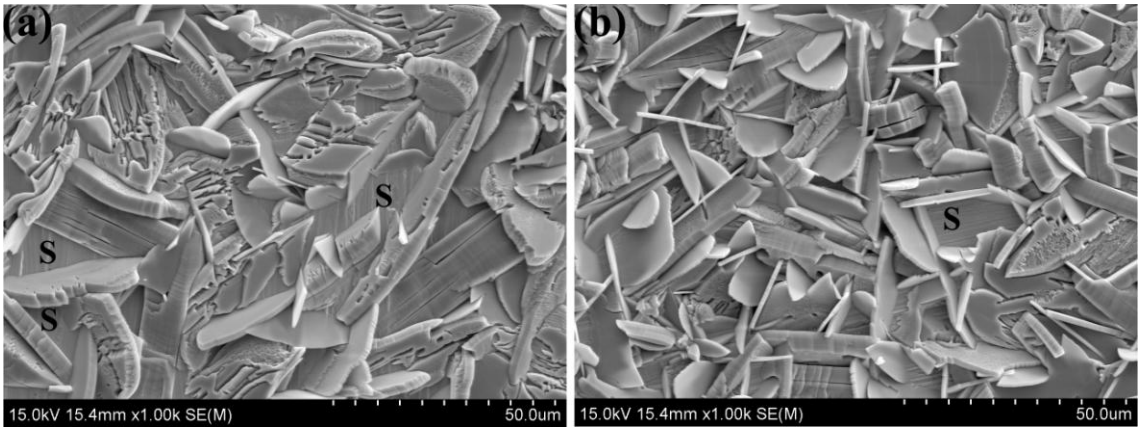


Fig. 4 FE-SEM images of the local high magnification in Fig. 3a and b. (S: Substrate)

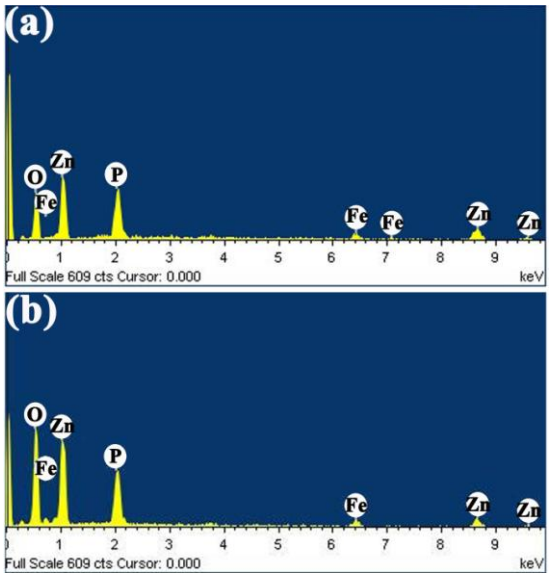


Fig. 5 EDS spectra of hopeite coatings by PCC treated at 75 ℃ for 30 min NSB (a) and with SB (b) substrates.

The inserted images in Fig. 3 e-f show microscopic features of one crystal surfaces, showing distinct nanoscale structures. These results are evidenced by AFM analysis, as shown in Fig. 6. The wavy profile is found on the crystal surface on NSB substrate with roughness of 16.2 nm (Fig. 6 a). The relatively uniform banded structure is exhibited on the crystal surface on SB substrate with roughness of 8.2 nm (Fig. 6 b). This may have

potential significance to biomedical application. Recently, hopeite has been considered a potential versatile biomedical material and cells attach and spread well on its surface [12, 17, 22]. Micro- and nano-scale structures of material surface affect cell adhesion and proliferation [31-33]. Meanwhile, hopeite coatings could present different scale ranges of topography, which is closely related to its cell and bone responses [13, 14].

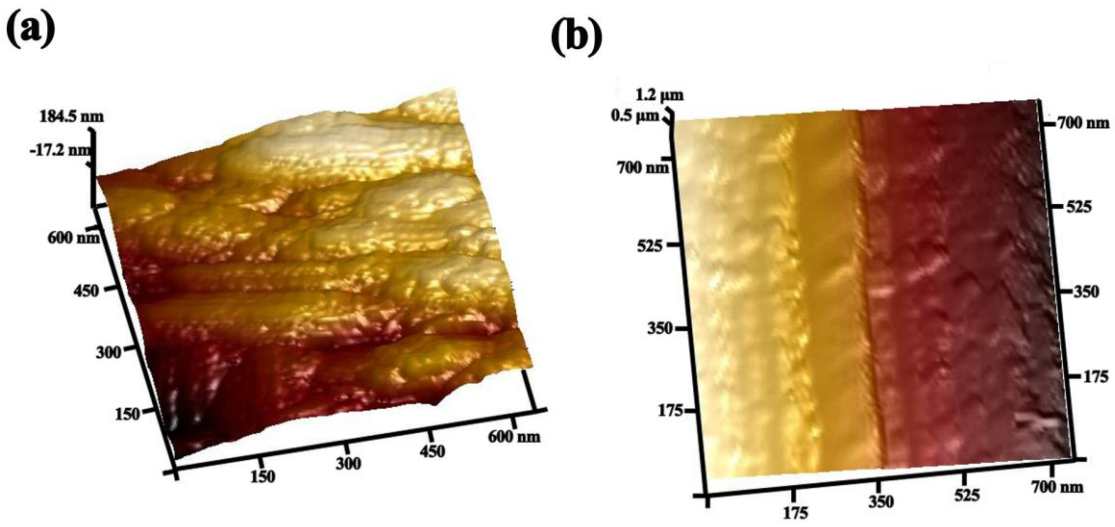


Fig. 6 Three-dimensional AFM images of crystal surface of coatings PCC treated at 75 ℃ for 30 min on NSB (a) and SB (b) substrates.

### 3.3 Electrochemical investigation

Fig. 7 demonstrates the potentiodynamic polarization curves of the PCC treated samples and uncoated 304 SS substrate. The electrochemical parameters used to evaluate the properties of the coating are calculated by the following equations by potentiodynamic polarization curves. The polarization resistance ($R_p$), which represents the corrosion properties of samples, was calculated using Equation (2) [34]:

$$R_p = \beta_a \times |\beta_c| / 2.303 I_{corr} \times (\beta_a + |\beta_c|) \quad (2)$$

where $R_p$ is the polarization resistance, $I_{corr}$ is the corrosion current density, $\beta_a$ is anodic Tafel slope and $\beta_c$ is cathode Tafel slope. The porosity percentage of PCC coating was calculated according to Equation (3) [35, 36]:

$$P = \left(R_{p,s}/R_p\right) \times 10^{-(\Delta E_{corr}/\beta_a)} \times 100\% \quad (3)$$

where $P$ is the total coating porosity percentage, $R_{p,s}$ is the polarization resistance of bare substrate, $R_p$ is the polarization resistance of coated substrate, $\Delta E_{corr}$ is the difference between corrosion potentials of coated and bare substrate, $\beta_a$ is anodic Tafel slope of the bare substrate. Finally, the corrosion protection efficiency was calculated using Equation (4) [37, 38]:

$$P_e = (1 - I_{corr}/I^0_{corr}) \times 100 \quad (4)$$

where $P_e$ is the corrosion protection efficiency of the coating, $I_{corr}$ and $I^0_{corr}$ are the corrosion current density of the coated sample and the substrate, respectively.

Table 1 summarizes the electrochemical parameters, such as corrosion potential ($E_{corr}$), corrosion current density ($I_{corr}$), polarization resistance ($R_p$), the porosity percentage ($P$) and the corrosion protection efficiency ($P_e$), of the substrate coated and uncoated coatings, which are calculated from Fig. 7 using the Tafel extrapolation method.

It is obviously seen that the polarization curves assigned for samples with coatings show a decrease of $I_{corr}$ and increase of $E_{corr}$ distinct as compared with those of NSB and SB substrates in a 0.9 wt. % sodium chloride solution, indicating the PCC coating has better corrosion resistance than uncoated substrates, resulted from uniform, fine and

compact microstructures as well as the chemical stability of phosphophyllite [10]. On the other hand, comparison between the curves of SB and NSB substrates indicates that the NSB substrate shows increase of $I_{corr}$ and decrease of $E_{corr}$. The SB substrate shows a poorer corrosion resistance, because of the existence of many active centers, dislocation on its surface [25, 27].

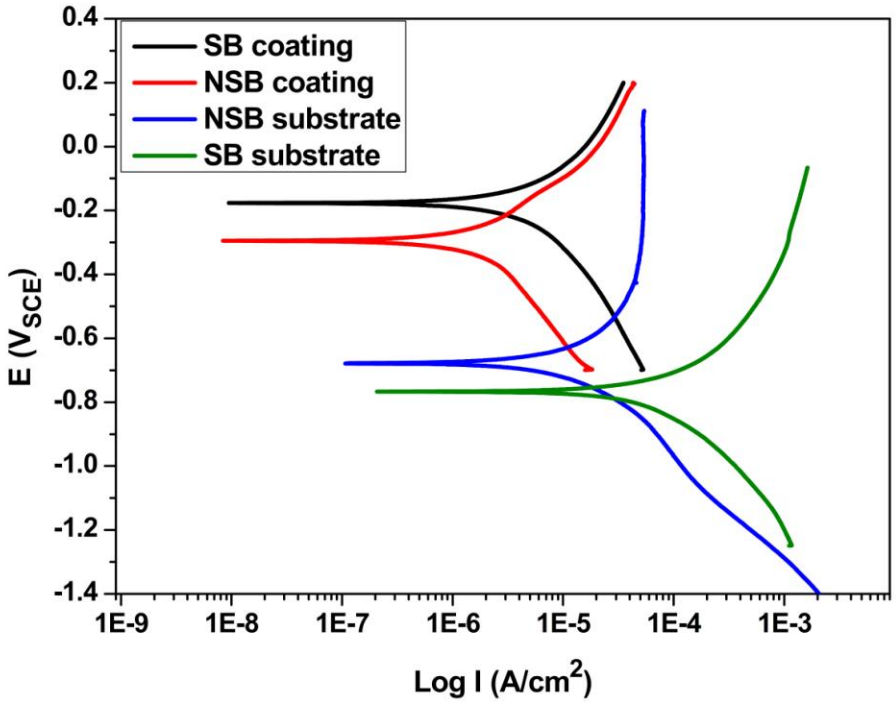


Fig. 7 Polarization curves for 304 SS samples PCC treated at 75 ℃ for 30 min and uncoated SB and NSB substrates in a 0.9 wt. % sodium chloride solution.

The PCC coatings treated for 30 min possess the low porosity percentage and high corrosion protection efficiency (Table 1), which will block the harmful ions to corrosion the substrate. It is seen that the porosity percentage and the corrosion protection efficiency of coatings on NSB and SB substrates have little difference. Compared with

the bare SB substrate, the $I_{corr}$ of the PCC coating decreases about 21 times and the $R_p$ increases about 4 times, while the $I_{corr}$ and $R_p$ of coating on NSB substrate are changed about 6 and 2 times to NSB substrate, respectively. Therefore, the PCC coating on SB substrate shows the greater corrosion protection performance than that on NSB substrate. This is due to the fact that the coating on SB substrate is denser with finer crystals (Fig. 5). Moreover, the higher thickness and coating mass provide better corrosion resistance for coating on SB substrate [10]. Apparently, on the basis of the above analysis, the advantage of the PCC coating on SB substrate over that on NSB substrate has been demonstrated.

Table 1 The results of potentiodynamic corrosion tests of the PCC treated sample at 75 ℃ for 30 min with and without SB treatment and bare substrate in a 0.9 wt. % sodium chloride solution.

| | $E_{corr}$ ($V_{SCE}$) | $I_{corr}$ ($\mu A/cm^2$) | $R_p$, $\times 10^3$ ($\Omega \cdot cm^2$) | $P$ (%) | $P_e$ (%) |
|---|---|---|---|---|---|
| NSB substrate | -0.38 | 9.84 | 2.62 | -- | -- |
| NSB coating | -0.19 | 0.74 | 7.45 | 1.63 | 84.65 |
| SB substrate | -0.47 | 76.8 | 0.23 | -- | -- |
| SB coating | -0.124 | 2.65 | 5.78 | 0.214 | 95.2 |

Note: NSB substrate means non-sandblasting substrate. NSB coating means hopeite coating PCC treated at 75 ℃ for 30 min on non-sandblasting substrate. SB substrate means sandblasting substrate. SB coating means hopeite coating PCC treated at 75 ℃ for 30 min on sandblasting substrate.

### 3.4 Adhesion test

According to the result of adhesion test, the determined tensile strength of coated

samples on substrate before and after sandblasting treatment, which are treated at 75 ℃ with bath pH of 2.75 for 30 min, between the ZPCC coating and the substrate is 17.01 ± 1.9 MPa and up to 21.19 ± 2.9 MPa,. The ZPCC coatings have been known as contiguous and porous, which could lead to the highly adherent between the organic coating and the substrate [10].

## 4. Conclusions

By developing a PCC coating on 304 SS, the effects of sandblasting on formation, microstructure and corrosion resistance of the hopeite coatings were investigated. Both the coatings on SB and NSB substrates had similar phase composition. Sandblasting treatment of substrate significantly decreased crystal size and increased crystallinity of the coating. The SB substrate was fully covered with the coating after PCC treatment for 1.5 min. The corrosion resistance of the PCC coating on SB substrate was significantly improved. Adhesive test indicated that the PCC coating was strongly attached on the substrate. The more uniform and finer PCC coating may have potential biomedical use due to the better corrosion resistance and the higher adhesive strength. Further studies such as biocompatibility are being undertaken.

## Acknowledgements

This work was supported by Shandong Provincial Natural Science Foundation of China (ZR2013EMM013),, Shandong Province Young and Middle-aged Scientists Research Awards Fund (BS2013CL030), Shandong Provincial Science and Technology Development Plan (2014GGX102031) and Independent Innovation Foundation of

Shandong University of China (2015JC018).

## References

1. M. Geetha, A. Singh, R. Asokamani and A. Gogia, *Prog. Mater. Sci.*, 2009, 54, 397-425.
2. O. Addison, A. Davenport, R. J. Newport, S. Kalra, M. Monir, J. F. W. Mosselmans, D. Proops and R. A. Martin, *J. R.Soc. Interface*, 2012, 3161-3164.
3. B. G. Pound, *Corros. Rev.*, 2014, 32, 21-41.
4. R. Okner, A. J. Domb and D. Mandler, *New J. Chem.*, 2009, 33, 1596-1604.
5. C. Y. Guo, A. T. Hong Tang, J. K. Hon Tsoi and J. P. Matinlinna, *J. Mech. Behav. Biomed.* , 2014, 32, 145-154.
6. Y. Song, D. Shan and E. Han, *Mater. Lett.*, 2008, 62, 3276-3279.
7. Y.-Y. Chang and D.-Y. Wang, *Sur. Coat. Technol.*, 2005, 200, 2187-2191.
8. T. Albrektsson, *J. Oral Maxil. Surg.*, 1998, 56, 1312-1326.
9. J. J. Lee, L. Rouhfar and O. R. Beirne, *J. Oral Maxil.l Surg.*, 2000, 58, 1372-1379.
10. T. S. Narayanan, *Rev. Adv. Mater. Sci*, 2005, 9, 130-177.
11. S. Shibli and A. Jayalekshmi, *Appl. Surf. Sci.*, 2008, 254, 4103-4110.
12. L. Herschke, J. Rottstegge, I. Lieberwirth and G. Wegner, *J. Mater. Sci-Mater. M.*, 2006, 17, 81-94.
13. R. A. Gittens, R. Olivares-Navarrete, A. Cheng, D. M. Anderson, T. McLachlan,

I. Stephan, J. Geis-Gerstorfer, K. H. Sandhage, A. G. Fedorov and F. Rupp, *Acta Biomater.*, 2013, 9, 6268-6277.

14. J. E. Davies, E. Ajami, R. Moineddin and V. C. Mendes, *Biomaterials*, 2013, 34, 3535-3546.

15. J. E. Davies, V. C. Mendes, J. C. Ko and E. Ajami, *Biomaterials*, 2014, 35, 25-35.

16. A. Valanezhad, K. Tsuru, M. Maruta, G. Kawachi, S. Matsuya and K. Ishikawa, *Bioceram. Dev. Appl.*, 2010, 1, 1-3.

17. A. Valanezhad, K. Tsuru, M. Maruta, G. Kawachi, S. Matsuya and K. Ishikawa, *Sur. Coat. Technol.*, 2012, 206, 2207-2212.

18. J. Flis, J. Mańkowski, T. Zakroczymski and T. Bell, *Corros. Sci.*, 2001, 43, 1711-1725.

19. A. Oskuie, A. Afshar and H. Hasannejad, *Sur. Coat. Technol.*, 2010, 205, 2302-2306.

20. A. Valanezhad, K. Tsuru, M. Maruta, G. Kawachi, S. Matsuya and K. Ishikawa, *Sur. Coat. Technol.*, 2010, 205, 2538-2541.

21. X. Zhang, G. Y. Xiao, Y. Jiao, X. C. Zhao and Y. P. Lu, *Sur. Coat. Technol.*, 2014, 240, 361-364.

22. X. C. Zhao, G. Y. Xiao, X. Zhang, H. Y. Wang and Y. P. Lu, *J. Phys. Chem. C*, 2014, 118, 1910-1918.

23. X. Zhang, G.-Y. Xiao, B. Liu, C.-C. Jiang and Y.-P. Lu, *New J. Chem.*, 2015, 39,

5813-5822.

24. X. Zhang, G.-Y. Xiao, C.-C. Jiang, B. Liu, N.-B. Li, R.-F. Zhu and Y.-P. Lu, *Corros. Sci.*, 2015, 94, 428-437.

25. A. Harris and A. Beevers, *Int. J. Adhes. Adhes.*, 1999, 19, 445-452.

26. K. Poorna Chander, M. Vashista, K. Sabiruddin, S. Paul and P. Bandyopadhyay, *Mater. Design*, 2009, 30, 2895-2902.

27. E. I. Ghali and R. Potvin, *Corros. Sci.*, 1972, 12, 583-594.

28. E. I. Ghali and R. J. A. Potvin, *Corrosion Science*, 1972, 12, 583-594.

29. L. Herschke, I. Lieberwirth and G. Wegner, *J. Mater. Sci-Mater. M.*, 2006, 17, 95-104.

30. G. Mangalam and S. J. Das, *Archives of Applied Science Research*, 2010, 1, 54-61.

31. F. Gentile, L. Tirinato, E. Battista, F. Causa, C. Liberale, E. M. Di Fabrizio and P. Decuzzi, *Biomaterials*, 2010, 31, 7205-7212.

32. M. Nikkhah, F. Edalat, S. Manoucheri and A. Khademhosseini, *Biomaterials*, 2012, 33, 5230-5246.

33. R. A. Gittens, T. McLachlan, R. Olivares-Navarrete, Y. Cai, S. Berner, R. Tannenbaum, Z. Schwartz, K. H. Sandhage and B. D. Boyan, *Biomaterials*, 2011, 32, 3395-3403.

34. C. Andrade and C. Alonso, *Mater. Struct.*, 2004, 37, 623-643.

35. V. de Freitas Cunha Lins, G. F. de Andrade Reis, C. R. de Araujo and T.

Matencio, *Appl. Surf. Sci.*, 2006, 253, 2875-2884.

36. J. Creus, H. Mazille and H. Idrissi, *Sur. Coat. Technol.*, 2000, 130, 224-232.

37. B.-L. Lin, J.-T. Lu and G. Kong, *Corros. Sci.*, 2008, 50, 962-967.

38. M. Fouladi and A. Amadeh, *Electrochimica Acta*, 2013, 106, 1-12.